

DFT-GGA errors in NO chemisorption energies on (111) transition metal surfaces: Possible origins and correction schemes

Xu Huang and Sara E. Mason
Department of Chemistry
University of Iowa, Iowa City, Iowa 52242
 (Dated: August 8, 2018)

Here we investigate whether well-known DFT-GGA errors in predicting the chemisorption energy (E_{chem}) of CO on transition metal surfaces manifest in analogous NO chemisorption systems. To verify the occurrence of DFT-GGA overestimation of the back-donation mechanism in NO chemisorption, we use electronic structure analysis to show that the partially filled molecular NO $2\pi^*$ orbital rehybridizes with the transition metal d -band to form new bonding and anti-bonding states. We relate the back-donation charge transfer associated with chemisorption to the promotion of an electron from the 5σ orbital to the $2\pi^*$ orbital in the gas-phase NO $G^2\Sigma^- \leftarrow X^2\Pi$ excitation. We establish linear relationships between E_{chem} and $\Delta E_{G\leftarrow X}$ and go on to formulate an E_{chem} correction scheme in the style of Mason *et al.*, [Physical Review B **69**, 161401(R)]. We apply the NO E_{chem} correction method to the (111) surfaces of Pt, Pd, Rh, and Ir, with NO chemisorption modeled at a coverage of 0.25 ML. We note that both the slope of E_{chem} *vs.* $\Delta E_{G\leftarrow X}$ and the dipole moment depend strongly on adsorption site for each metal, and we use this fact to construct an approximate correction scheme which we go on to test using NO/Pt(100) chemisorption.

I. INTRODUCTION

The chemisorption of nitric oxide (NO) and carbon monoxide (CO) on transition metal surfaces has drawn much research attention due to the fundamental importance of these processes to applications in catalysis. In this study, we focus on the issue of density functional theory (DFT) predictions of the chemisorption energy, E_{chem} , of NO on transition metal surfaces. In particular, we investigate whether well-known shortcomings in DFT predictions for E_{chem} of CO manifest in NO/metal systems. This so-called ‘‘CO/metal puzzle’’ [1] can be summarized as the tendency for generalized gradient approximation (GGA) functionals (such as PW91 [2], PBE [3] and RPBE [4]) to place the empty CO $2\pi^*$ orbital too low in energy relative to the metal d -band. This results in an unrealistic strengthening of the $2\pi^*$ - d -band interaction, which is reflected in an overestimation of the chemisorption bond strength.

Further insight into the CO/metal puzzle can be obtained by considering the Hammer-Morikawa-Norskov (HMN) model for the d -band contribution to CO E_{chem} [5]. The back-donation term, $E_{\text{chem}}^{d\rightarrow 2\pi^*}$, thought to dominate chemisorption on late transition metal surfaces, is given by:

$$E_{\text{chem}}^{d\rightarrow 2\pi^*} = \frac{-4fV_{\pi}^2}{(\epsilon_{2\pi^*} - \epsilon_d)} \quad (1)$$

where f is the idealized filling of the metal d band, V_{π}^2 is the NO π -surface coupling matrix element, $\epsilon_{2\pi^*}$ is the energy of the renormalized $2\pi^*$ orbital relative to the Fermi level, and ϵ_d is the first moment of the metal d -projected density of states relative to the Fermi level. The HMN model predicts that larger values of V_{π}^2 give rise to greater back-donation, and based on overlap arguments V_{π}^2 is expected to increase with the extent of

CO-metal coordination. As shown in Figure 1, the (111) surface of fcc transition metals has four high-symmetry adsorption sites, which in order of increasing coordination are top (T) < bridge (B) < hcp hollow (H) = fcc hollow (F). Thus, based on the HMN model interpretation of the CO/metal puzzle, the 3-fold H and F sites will exhibit greater DFT-GGA overestimation of $E_{\text{chem}}^{d\rightarrow 2\pi^*}$ than the doubly coordinated B site or singly coordinated T site.

Several studies have traced the CO/metal puzzle to its origins [6–8], and various schemes have been developed to correct or address it [8–11]. One approach, a post-DFT extrapolation procedure, was developed by Grinberg and Rappe in collaboration with one of the co-authors of this study [12]. The extrapolation procedure was based on the linear relationship between E_{chem} and the CO singlet-triplet excitation energy $\Delta E_{T\leftarrow S}$, and was developed for different adsorption sites on (111) and (100) transition metal surfaces of Pt, Pd, Rh, and Cu. The linear trends were determined by changing the design of carbon and oxygen pseudopotentials sufficiently to achieve variation in the predicted properties. The linear trends obtained from the DFT-GGA calculations were then extrapolated to a $\Delta E_{T\leftarrow S}$ value from a configuration interaction calculation. Finally, the corresponding ordinates were taken to be the corrected values of E_{chem} . Consistent with the above conceptual argument that the DFT-GGA error in $E_{\text{chem}}^{d\rightarrow 2\pi^*}$ will be larger for higher NO-metal coordination, the slope $\delta E_{\text{chem}}^{\text{GGA}} / \delta \Delta E_{T\leftarrow S}^{\text{GGA}}$ was found to have the greatest magnitude at hollow sites and the smallest magnitude at top sites.

The accuracy of DFT-GGA predictions of E_{chem} for NO on transition metals has been given less consideration than in the analogous case of CO. This may be due in part to the fact that CO preferentially adsorbs at top sites on several late transition metal surfaces. As the nature of the CO/metal puzzle is to overestimate E_{chem} at

highly coordinated sites more than at top sites, this leads to cases of incorrect site preference predictions for CO in uncorrected DFT-GGA calculations [7, 13–15]. On the other hand, NO exhibits an inherent preference to adsorb at highly coordinated sites on most late transition metal surfaces. Therefore, the same overestimation of back-donation in NO/metal systems will not result in the gross qualitative error of incorrect site preference as seen in many CO/metal systems. Instead, overestimation of $E_{\text{chem}}^{d \rightarrow 2\pi^*}$ in NO/metal systems will only manifest quantitatively in calculated values of E_{chem} , in a site-specific fashion. In addition to there being no obvious problem with DFT-GGA predictions of NO site preference, there are theoretical arguments for why overestimation of back-donation may not occur. For example, in a comprehensive DFT study [16], a detailed comparison of CO and NO chemisorption is presented, and it is suggested that the partial occupation of the NO $2\pi^*$ orbital effectively “pins” the energy of that state to the Fermi level, which prevents overestimation of back-donation.

In the present study, we demonstrate that in most adsorption geometries, the rehybridization of the NO $2\pi^*$ orbital in the chemisorbed state can give rise to new bonding and anti-bonding states. The NO/metal $2\pi^*$ rehybridization is compared to that in CO/metal systems, and we interpret the results to support that DFT-GGA overestimation of $E_{\text{chem}}^{d \rightarrow 2\pi^*}$ does affect predictions for E_{chem} in NO/metal systems. We demonstrate a linear relationship between NO E_{chem} and $\Delta E_{G \leftarrow X}$, the energy of the $G^2\Sigma^- \leftarrow X^2\Pi$ excitation of the free NO molecule. We use these findings as the basis for the development of a post-DFT extrapolation scheme in the style of Mason and co-workers [12]. Corrected values for E_{chem} do not in general affect the predicted NO site preference, but do quantitatively change the values of E_{chem} by up to 18%.

II. METHODOLOGY

Calculations are carried out using an in-house solid state DFT code as used in previous studies [12, 17–19] employing the PBE-GGA exchange-correlation functional. Norm-conserving optimized (RRKJ) [20] pseudopotentials with the designed nonlocal method for metals [21] or Troullier and Martins (TM) style [22] norm-conserving pseudopotentials are employed, generated using the OPIUM pseudopotential package [23]. In all DFT calculations, the Kohn-Sham orbitals are expanded in a plane-wave basis set truncated at 50 Ry.

NO Chemisorption is modeled on the (111) surfaces of Rh, Pd, Ir and Pt. The theoretical lattice constants of face-centered unit cell for those metal species are determined to be 3.797, 3.867, 3.840 and 3.954 Å, respectively, based on polynomial fits and minimization of primitive bulk cell total energy *vs.* volume data points. Models for the (111) surfaces are generated in $c(4 \times 2)$ supercells (shown in Figure 1) comprised of five atomic layers of metal and at least 15.6 Å of vacuum separating periodic

images in the surface normal direction. In all surface calculations, the first Brillouin zone is sampled using a converged $4 \times 4 \times 1$ grid of Monkhorst-Pack k -points [24]. NO chemisorption is modeled at 1/4 ML coverage in each of the four adsorption sites T, B, H, and F (Figure 1), with NO bonding perpendicular to the surface (except as noted) and through N. Geometry optimization for each structure, allowing for relaxation in the top two metal layers, is performed until the highest residual force is no larger than 0.01 eV/Å. For the T site, two sets of calculations are carried out, either imposing linear (T_1) or allowing for bent (T_b) chemisorbed NO geometries.

In order to track changes in values of E_{chem} with variations in molecular NO electronic structure, calculations of the NO/metal systems using 4 distinct O pseudopotentials are carried out, with details of the O pseudopotential designs given in Table I.

Values for E_{chem} are calculated using

$$E_{\text{chem}} = E_{\text{NO/surface}} - E_{\text{NO}} - E_{\text{surface}}. \quad (2)$$

With this definition, chemisorption energies are reported in eV/NO molecule, and negative values of E_{chem} represent favorable adsorption on the surface.

Atomic state-by-state projected density of states (PDOS) analysis is carried out by projecting atomic valence pseudo-wavefunctions (radial wavefunction multiplied by real combination of spherical harmonics) of atoms onto all the Kohn-Sham orbitals. Band centers are then calculated as the first moment of each projection. Here, we are interested in monitoring how the states of NO change in going from the free molecule to the chemisorbed state. To approximate the projection onto NO π and σ orbitals, we follow the approach of Zeng and co-workers [25] and take linear combinations of N and O PDOS:

$$\pi = N_{p_x} + N_{p_y} + O_{p_x} + N_{p_y}, \quad (3)$$

$$\sigma = N_s + N_{p_z} + O_s + N_{p_z}. \quad (4)$$

III. RESULTS AND DISCUSSION

In our calculation using the O pseudopotential labeled PSP 1 in Table I, the N-O bond length, $d_{\text{N-O}}$ of the free NO molecule is 1.148 Å. This is in good agreement with the experimental value of 1.154 Å, though notably shorter than other DFT-GGA calculated results between 1.16 Å and 1.18 Å [16, 26–34]. We attribute the difference in $d_{\text{N-O}}$ to pseudopotential style, as the above referenced DFT-GGA values are all obtained using ultrasoft pseudopotentials, while our study employs norm-conserving optimized pseudopotentials. The values for $d_{\text{N-O}}$ and other aspects of the optimized NO/metal geometries using O PSP 1 are presented in Table II. For each metal

surface and site, d_{N-O} is up to 3.4% shorter than literature values for studies employing ultrasoft pseudopotentials [32, 33, 35–39], supporting systematic disagreement in d_{N-O} between the two pseudopotential approximations. For all metals, as expected, d_{N-O} increases with increasing NO-metal coordination. Chemically speaking, the bond order of chemisorbed NO decreases as d_{N-O} increases.

As shown in Figure 2, calculations for E_{chem} using the four distinct O pseudopotentials exhibit a linear relationship between E_{chem} and $\Delta E_{G\leftarrow X}$, similar to the linear relationships previously reported between CO E_{chem} and $\Delta E_{T\leftarrow S}$ [12] or CO E_{chem} and the energy of the CO $2\pi^*$ orbital [8]. The reason for the correlation between NO E_{chem} and $\Delta E_{G\leftarrow X}$ is considered in terms of the charge transfer in the chemisorption and molecular excitation processes. The $G^2\Sigma^- \leftarrow X^2\Pi$ excitation involves electron transfer from the NO 5σ orbital to $2\pi^*$ orbital, while back-donation in chemisorption involves charge transfer from the metal d -band into the $2\pi^*$ -derived bonding states.

In a style similar to Mason *et al.* [12], we extrapolate corrected values of the chemisorption energy $E_{\text{chem}}^{\text{corr}}$, as shown in Figure 2. The extrapolation process to calculate $E_{\text{chem}}^{\text{corr}}$ is summarized as

$$E_{\text{chem}}^{\text{corr}} = E_{\text{chem}} + (\Delta E_{G\leftarrow X}^{\text{exp}} - \Delta E_{G\leftarrow X}^{\text{GGA}}) \frac{\delta E_{\text{chem}}}{\delta \Delta E_{G\leftarrow X}^{\text{GGA}}}, \quad (5)$$

where $\Delta E_{G\leftarrow X}^{\text{exp}}$ and $\Delta E_{G\leftarrow X}^{\text{GGA}}$ are the experimental and DFT-GGA values for the NO $G^2\Sigma^- \leftarrow X^2\Pi$ excitation, respectively. Here, we use a reported experimental value for $\Delta E_{G\leftarrow X}$ 62913.0 cm^{-1} (7.80 eV) as the calibration [40]. $\delta E_{\text{chem}} / \delta \Delta E_{G\leftarrow X}^{\text{GGA}}$ indicates the so-called correction slope of the linear trend. All the $E_{\text{chem}}^{\text{corr}}$ results are given in Table III, alongside the uncorrected E_{chem} values obtained using O PSP 1.

An overall picture presented by Figure 2 and Table III is that values of $E_{\text{chem}}^{\text{corr}}$ are smaller in magnitude than uncorrected E_{chem} , and the correction slope has a significant dependence on the adsorption site. The trends in $\delta E_{\text{chem}} / \delta \Delta E_{G\leftarrow X}^{\text{GGA}}$ by site can be rationalized in terms of NO-metal coordination and how the orbitals of adsorbate and substrate overlap. As discussed in the literature [16, 25], for T_1 adsorption, the greatest contribution to the NO-metal overlap is from the 5σ orbital of NO molecule (comprised of N and O atomic s and p_z orbitals), and the d_{z^2} -derived states of the chemisorbing surface atom. When there are two or three surface atoms coordinated with NO, such as at B, H, or F sites, the metal atom-N-O angle is not linear, and this change in chemisorption geometry results in different dominant overlap interactions. Specifically, in B, H, or F geometries, the NO-metal overlap is dominated by interaction of the NO $2\pi^*$ orbital (comprised of N and O atomic p_x and p_y orbitals), and the d_{xz} - and d_{yz} -derived states of the chemisorbing surface atoms. Thus, as NO-metal coordination increases, the overlap between NO $2\pi^*$ and

the surface also increases, which causes the chemisorption bond to have more back-donation character. This leads to overestimation of $E_{\text{chem}}^{d\rightarrow 2\pi^*}$, the relative extent of which can be tracked by the relative values of $\delta E_{\text{chem}} / \delta \Delta E_{G\leftarrow X}^{\text{GGA}}$ for different sites.

As foreshadowed, the result of extrapolating to $E_{\text{chem}}^{\text{corr}}$ does not impact the predicted NO site preference in most cases, but does affect the magnitude of E_{chem} by up to 18%. The most favorable site before and after the correction is indicated in Table III. The one instance of altered site preference is for Ir(111), and this can be explained by the very close spacing of uncorrected E_{chem} values on that surface. Qualitatively, our results for site preference are in agreement with previous theoretical results [16, 25–39, 41–47]. Quantitatively, the values of $E_{\text{chem}}^{\text{corr}}$ reported here may be more reliable, and in particular the relative values of $E_{\text{chem}}^{\text{corr}}$ at different sites on the same metal may be important for interpreting how chemisorption evolves with coverage. For example, in the uncorrected values, the range of E_{chem} for different sites on Rh(111) is 0.584 eV, while the range in $E_{\text{chem}}^{\text{corr}}$ is 0.310. Thus the corrected values predict a much smoother potential energy surface than the uncorrected values.

The basis of our assertion that there is DFT-GGA overestimation of $E_{\text{chem}}^{d\rightarrow 2\pi^*}$ relies on the NO $2\pi^*$ orbital hybridizing with the surface d -band to form new bonding and anti-bonding states in the NO/metal system, similar to as seen in CO chemisorption. This is at odds with the conclusion reported by Gajdos and co-workers [16], which alternatively states that the NO $2\pi^*$ -derived states in NO/metal systems span a single, narrow energy range close to the Fermi level. In order to clarify the bonding interactions in NO/metal systems, we carry out comparative density of states analysis. In Figure 3, the projections onto the Pt d , NO π , and NO σ states is shown for NO/Pt(111) T_1 and F sites. Consistent with the interpretation of Gajdos *et al.*, inspection of the PDOS for the T_1 site shows that the $2\pi^*$ state, which we assign as the narrow and intense peak in the NO π PDOS just above the Fermi level, does not significantly hybridize with the Pt d -band. However, in the PDOS of the F configuration, the sharp peak in the NO π projection near the Fermi level is diminished, and new broad intensity appears at bonding energies of 0-4 eV below the Fermi level. Thus the PDOS provides evidence of charge transfer from the surface into NO $2\pi^*$ -derived states at the F site, which also gives rise to a relatively large correction slope value of 0.19. On the other hand, the absence of PDOS evidence for $2\pi^*$ -Pt hybridization in the T_1 geometry is reflected in the negligible value of $\delta E_{\text{chem}} / \delta \Delta E_{G\leftarrow X}$ for the T_1 site.

For comparison, the PDOS of CO/Pt(111) T_1 and F are presented in Figure 3. A key distinction between the PDOS of NO/Pt(111) and CO/Pt(111) is noted for the T_1 configurations: In CO/Pt(111) T_1 , the CO $2\pi^*$ state does hybridize with the surface, while this behavior is absent in the NO/Pt(111) T_1 . The fact that hybridization of the molecular $2\pi^*$ states occurs at the F site but does

not occur at the T_1 site in NO/Pt(111) may be why it has been previously thought that NO/metal systems are not subject to the same overestimation of $E_{\text{chem}}^{d \rightarrow 2\pi^*}$ as confirmed in CO/metal systems. The PDOS for NO/Pt(111) B and H sites, not shown, show behavior qualitatively similar to NO/Pt(111) H.

The chemisorption-induced charge transfer is further investigated by studying the changes in the occupation of NO and CO π and σ states between the gas-phase and chemisorbed systems. Using an analysis similar to as done by Zeng and co-workers, [25] fractional fillings of the chemisorbed NO σ and π projections are calculated and compared to the ideal molecular values. The changes in π occupation, $\Delta\pi$, and in σ occupation, $\Delta\sigma$, are reported in Table IV, along with the sum net change in both occupations. For all of the NO and CO chemisorption systems, the positive values of $\Delta\pi$ reflect increased occupation of the π states upon chemisorption, while the negative values of $\Delta\sigma$ reflect decreased occupation of the σ states. The magnitude of $(\Delta\pi + \Delta\sigma)$ increases with NO-metal coordination. The trends in $\Delta\pi$ and $\Delta\sigma$ for NO and CO support that simultaneous donation and back-donation contribute to the chemisorption process of both molecules, in agreement with other theoretical descriptions of NO (as in References [25, 28, 32]) and CO (as in References [5, 27]) chemisorption. Comparing the NO/Pt(11) and CO/Pt(111) systems, the larger $\Delta\pi$ values of the latter may be attributed to the empty occupation of the molecular CO $2\pi^*$ orbital. The comparative values of $\Delta\pi$ are also consistent with the relative magnitude of the correction slopes in NO and CO systems. For example, as previously reported for CO, the correction slopes for Rh, Pd and Pt(111) surfaces can be up to 0.26 for top site and 0.56 for hollow site [12], while in this work that the correction slopes are near 0 for T_1 sites and up to 0.25 for H and F sites (Table III).

The presented correction scheme requires calculations using multiple pseudopotentials to determine the values of $\delta E_{\text{chem}} / \delta \Delta E_{G \leftarrow X}$. In the CO extrapolation procedure, it was noted that the correction slope values correlated with the CO vibrational stretch frequency values for each site, with little dependence on the metal identity. While this afforded an approximate correction scheme for CO/metal systems, the overlapping ranges for the NO vibrational stretch frequency values at different sites as discussed in References [16] and [48] precludes such a short-cut for approximating $\delta E_{\text{chem}} / \delta \Delta E_{G \leftarrow X}$. However, we note that there is a correlation between the correction slope and calculated dipole moment, μ . Here we define the electron distribution of $N^{\delta-}-O^{\delta+}$ as positive dipole moment, and $N^{\delta+}-O^{\delta-}$ as negative dipole moment. As recently reported and interpreted by Deshlahra and co-workers [46], the sign and magnitude of the dipole moment of values in NO/metal exhibits site-specific trends, with T sites having $\mu > 0$, and H sites having $\mu < 0$. The Pt(111) correction slopes for the five (111) adsorption sites and associated values of μ are given in Table V. As shown in Figure 5, our calculated values of μ demon-

strate that the sign of μ changes from positive to negative as the NO-metal coordination increases. Simultaneously, the correction slopes grow larger, consistent with the greater extent of back-donation at highly coordinated adsorption sites.

The relationship between μ and $\delta E_{\text{chem}} / \delta \Delta E_{G \leftarrow X}$ enables an approximate scheme for determining correction slope. In this way, $E_{\text{chem}}^{\text{corr}}$ can be extrapolated using a smaller set of DFT calculations. To test the μ -based extrapolation scheme, we model the NO/Pt(100) chemisorption system and determine $E_{\text{chem}}^{\text{corr}}$ in two ways, first using the full extrapolation procedure and again by using the μ -based correction detailed below. Chemisorption energies using the μ -based correction are denoted $E_{\text{chem}}^{\text{corr,dip}}$. This comparison is done for three adsorption sites on Pt(100) surfaces shown in Figure 4: top (T), bridge (B), and the four-fold hollow site H_4 .

To carry out the dipole-based correction method, we first calculate E_{chem} and the corresponding dipole moment for NO at the three sites on Pt(100) using O PSP 1. The NO/Pt(100) values of μ are used along with the NO/Pt(111) trend between μ and $\delta E_{\text{chem}} / \delta \Delta E_{G \leftarrow X}$ to approximate the NO/Pt(100) correction slope for each site. Once the value of $\delta E_{\text{chem}} / \delta \Delta E_{G \leftarrow X}$ is approximated, the correction method proceeds in the same fashion as detailed for the full method, using an experimental value for $\Delta E_{G \leftarrow X}$ to arrive at values of $E_{\text{chem}}^{\text{corr,dip}}$. We suggest a range of NO/Pt(100) correction slope values based on the dipole correlation, and in Figure 6 the resulting upper and lower bound $E_{\text{chem}}^{\text{corr}}$ values are shown. Before correction, the E_{chem} value for the Pt(100) bridge site (reported as the preferred geometry [49–52]) is -2.109 eV; after correction, the range of $E_{\text{chem}}^{\text{corr,dip}}$ is -1.913 eV to -1.951 eV. As a comparison, the full pseudopotential correction method is also performed and plotted in Figure 6. The result of -1.937 eV obtained from the full correction scheme is within the bounds of the dipole-based approximate correction method, supporting the validity and utility of the μ -based correction. Results for the remaining NO/Pt(100) sites using both the full and μ -based correction method are given in Table V.

IV. CONCLUSIONS

NO chemisorption on Rh, Pd, Ir, and Pt(111) surfaces is studied to assess if over-estimation of back-donation leads to systematic errors in DFT-GGA predictions for E_{chem} . The electronic structure of NO/metal and CO/metal systems shows that, with the exception of linear top site adsorption, the NO $2\pi^*$ orbital does rehybridize with the surface d -band to form new bonding and anti-bonding states, similar to what is seen in the analogous CO/metal systems. Linear trends of NO E_{chem} vs. $\Delta E_{G \leftarrow X}$ are obtained by calculations utilizing different O pseudopotentials, and a post-DFT correction scheme for NO E_{chem} is constructed after the style of a CO chemisorption energy extrapolation procedure [12].

In the case of NO, the E_{chem} correction does not impact the predicted site preference. However, as the impact of the correction varies with adsorption site, the relative values of E_{chem} for different sites on a given metal are affected. In most cases, the corrected values predict smoother NO/metal potential energy surfaces than the uncorrected values. The implication of the correction could be meaningful in understanding the evolution of NO chemisorption with coverage, NO diffusion on surfaces, or for accurately predicting the relative magnitude of E_{chem} in NO/metal systems.

V. ACKNOWLEDGMENTS

S.E.M. thanks the University of Iowa College of Liberal Arts and Sciences and the Iowa Center for Research by Undergraduate for funding this work. We thank Prof. Andrew M. Rappe and his research group for use of an in-house DFT code and for the online availability of RRKJ transition metal pseudopotential design details. Daniel J. Gillette is acknowledged for carrying out geometry optimization calculations contributing to this project.

TABLE I: Details of oxygen pseudopotential design. Core radii r_c for the O s and p are in a_o . All pseudopotentials were created using 50 Ry cutoff energy, and from the s^2p^4 reference configuration. For each pseudopotential, the norm-conserving pseudopotential type (RRKJ [20] or TM[22]) and associated values of $\Delta E_{G\leftarrow X}^{\text{GGA}}$ in eV are given.

	Type	r_{c^s}, r_{c^p}	$\Delta E_{G\leftarrow X}^{\text{GGA}}/\text{eV}$
PSP 1	TM	1.34, 1.53	6.432
PSP 2	RRKJ	1.32, 1.44	6.519
PSP 3	RRKJ	1.34, 1.46	6.534
PSP 4	RRKJ	1.34, 1.53	6.558

TABLE II: Details of the optimized geometries of NO chemisorption obtained using O PSP 1. Reported values include the bond length between N and O, $d_{\text{N-O}}$, the average distance between N and coordinated surface metal atom(s), $d_{\text{N-TM}}$, and the vertical distance between N and the average height of the topmost metal surface layer, $h_{\text{N-TM}(111)}$.

	Site	$d_{\text{N-O}} / \text{\AA}$	$d_{\text{N-TM}} / \text{\AA}$	$h_{\text{N-TM}(111)} / \text{\AA}$
Rh(111)	T ₁	1.154	1.744	1.972
	B	1.183	1.931	1.464
	H	1.200	2.001	1.282
	F	1.200	2.008	1.295
Pd(111)	T ₁	1.152	1.806	1.949
	T _b	1.161	1.843	2.032
	B	1.177	1.927	1.426
	H	1.191	1.991	1.249
	F	1.194	1.987	1.227
Ir(111)	T ₁	1.153	1.757	1.991
	B	1.183	1.996	1.535
	H	1.203	2.067	1.355
	F	1.203	2.078	1.377
Pt(111)	T ₁	1.150	1.836	2.012
	T _b	1.158	1.940	2.131
	B	1.174	2.003	1.518
	H	1.187	2.098	1.359
	F	1.192	2.087	1.321

TABLE III: Results of linear regression of chemisorption energy *vs.* NO $\Delta E_{G\leftarrow X}$, dipole moment μ , and μ -based correction details for NO/Pt(100). The DFT-GGA values for E_{chem} are given, along with the corrected energies obtained by extrapolation, $E_{\text{chem}}^{\text{corr}}$. For convenience, the correction change in E_{chem} (obtained from O PSP 1), Δ , is listed. For each surface, the predicted preferred site is indicated by E_{chem} values in boldface.

	Site	Slope	$E_{\text{chem}}/\text{eV}$	$E_{\text{chem}}^{\text{corr}}/\text{eV}$	Δ/eV
Rh(111)	T ₁	0.024	-1.945	-1.912	0.033
	B	0.153	-2.298	-2.089	0.209
	H	0.224	-2.529	-2.222	0.307
	F	0.225	-2.463	-2.156	0.307
Pd(111)	T ₁	0.003	-1.179	-1.175	0.004
	T _b	0.051	-1.463	-1.393	0.070
	B	0.114	-1.883	-1.728	0.155
	H	0.178	-2.173	-1.930	0.243
	F	0.190	-2.207	-1.947	0.260
Ir(111)	T ₁	0.030	-1.955	-1.914	0.041
	B	0.160	-1.887	-1.668	0.219
	H	0.245	-1.986	-1.651	0.335
	F	0.249	-1.928	-1.587	0.341
Pt(111)	T ₁	-0.002	-0.984	-0.986	-0.002
	T _b	0.046	-1.408	-1.345	0.063
	B	0.106	-1.509	-1.363	0.146
	H	0.161	-1.543	-1.323	0.220
	F	0.187	-1.659	-1.403	0.256

TABLE IV: Calculated chemisorption-induced changes in the NO π and σ fillings, $\Delta\pi$ and $\Delta\sigma$, in NO/metal configurations relative to the respective gas-phase molecules.

	Site	$\Delta\pi$	$\Delta\sigma$	$\Delta\pi + \Delta\sigma$
NO/Rh(111)	T ₁	1.04	-0.93	0.11
	B	1.26	-0.99	0.27
	H	1.16	-0.77	0.39
	F	1.17	-0.77	0.39
NO/Pd(111)	T ₁	0.98	-1.00	-0.01
	T _b	0.63	-0.43	0.20
	B	1.23	-0.99	0.23
	H	1.15	-0.78	0.36
NO/Ir(111)	T ₁	1.06	-0.91	0.15
	B	1.37	-1.05	0.32
	H	1.20	-0.72	0.48
	F	1.22	-0.71	0.50
NO/Pt(111)	T ₁	1.00	-0.96	0.05
	T _b	0.63	-0.26	0.36
	B	1.40	-1.02	0.38
	H	1.23	-0.69	0.54
CO/Pt(111)	T ₁	1.57	-0.49	1.08
	T _b	1.57	-0.49	1.08
	B	1.69	-0.37	1.33
	H	1.69	-0.46	1.23
	F	1.68	-0.47	1.21

TABLE V: Results of linear regression of chemisorption energy *vs.* NO $\Delta E_{G\leftarrow X}$. The DFT-GGA values for E_{chem} and corresponding dipole moments μ (obtained from O PSP 1) are given, along with the suggested range of correction slope values Δm . The resulting range of μ -based $E_{\text{chem}}^{\text{corr}}$ and changes relative to uncorrected energies Δ^{dip} are listed. For comparison, the $E_{\text{chem}}^{\text{corr}}$ obtained from the full correction method are also given. For each surface, the predicted preferred site is indicated by E_{chem} values in boldface.

	Site	$\mu/e \text{ \AA}$	E_{chem}/eV	Δm	Range of $E_{\text{chem}}^{\text{corr,dip}}/eV$	Δ^{dip}/eV	$E_{\text{chem}}^{\text{corr}}/eV$
Pt(100)	T ₁	0.171	-1.420	[-0.035, -0.008]	[-1.468, -1.431]	[-0.048, -0.011]	-1.431
	B	0.021	-2.109	[0.116, 0.143]	[-1.951, -1.914]	[0.158, 0.195]	-1.937
	Hol	-0.013	-1.472	[0.149, 0.177]	[-1.268, -1.230]	[0.204, 0.242]	-1.246

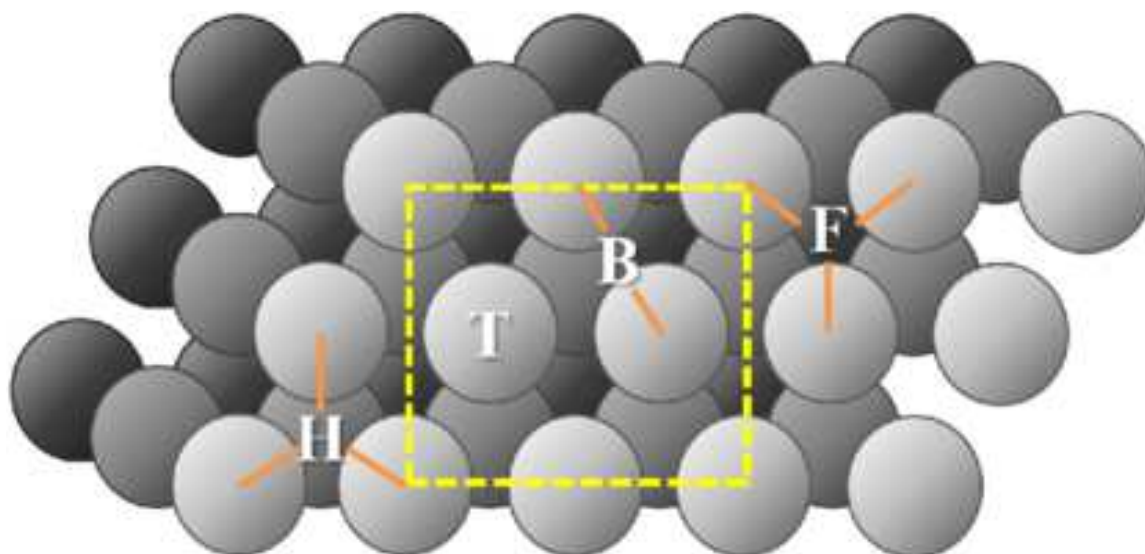


FIG. 1: Top view of the (111) fcc transition metal surface with high-symmetry adsorption site labels. Top (T), bridge (B), hcp (H), fcc (F) sites are labeled. The $c(4 \times 2)$ cell is indicated by dashed lines.

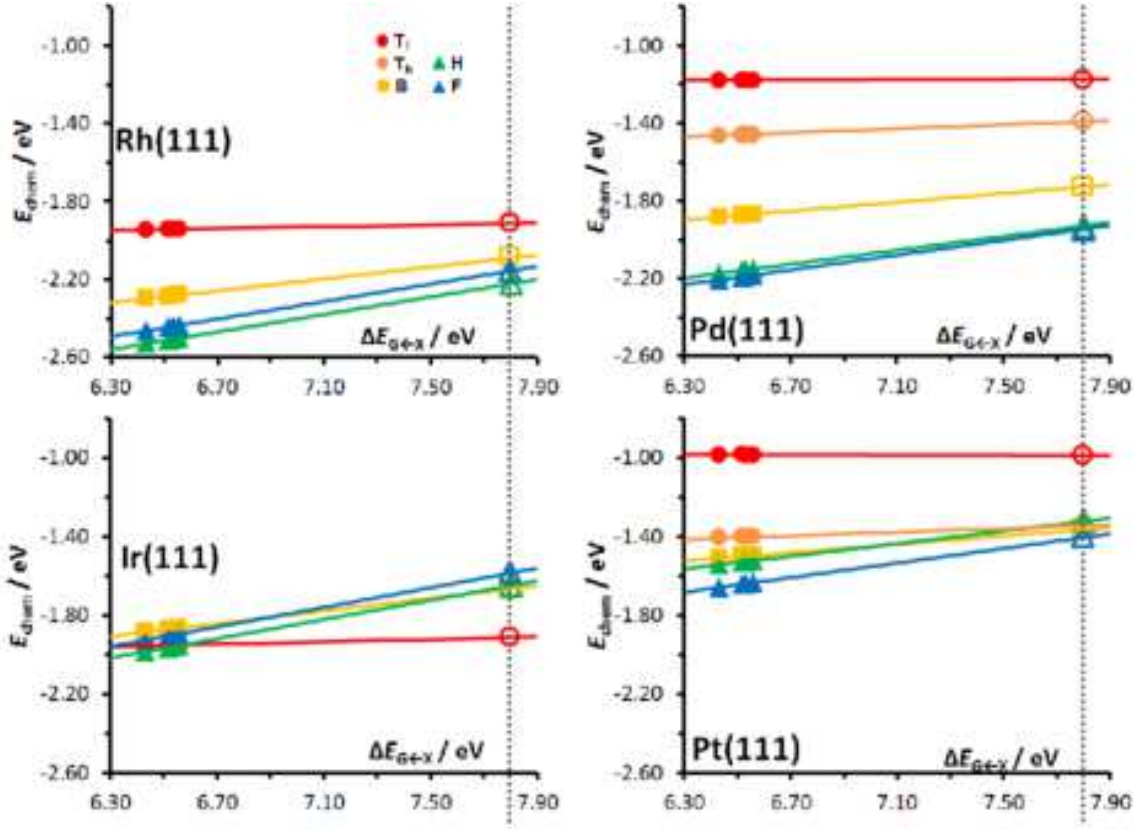


FIG. 2: (Color online) Plots of E_{chem} vs. $\Delta E_{G \leftarrow X}$ for calculations using the four sets of O pseudopotentials (in Table I) for 1/4 ML NO at T_l (red circles), T_b (orange circles), B (yellow squares), H (green triangles), and F (blue triangles) sites on Rh, Pd, Ir, and Pt(111) surfaces. Values of E_{chem} are indicated by filled symbols, while the corresponding values of $E_{\text{chem}}^{\text{corr}}$ are shown by open symbols. The experimental value for $\Delta E_{G \leftarrow X}$ 62913.0 cm^{-1} (7.80 eV) is indicated in each plot by a vertical dotted line.

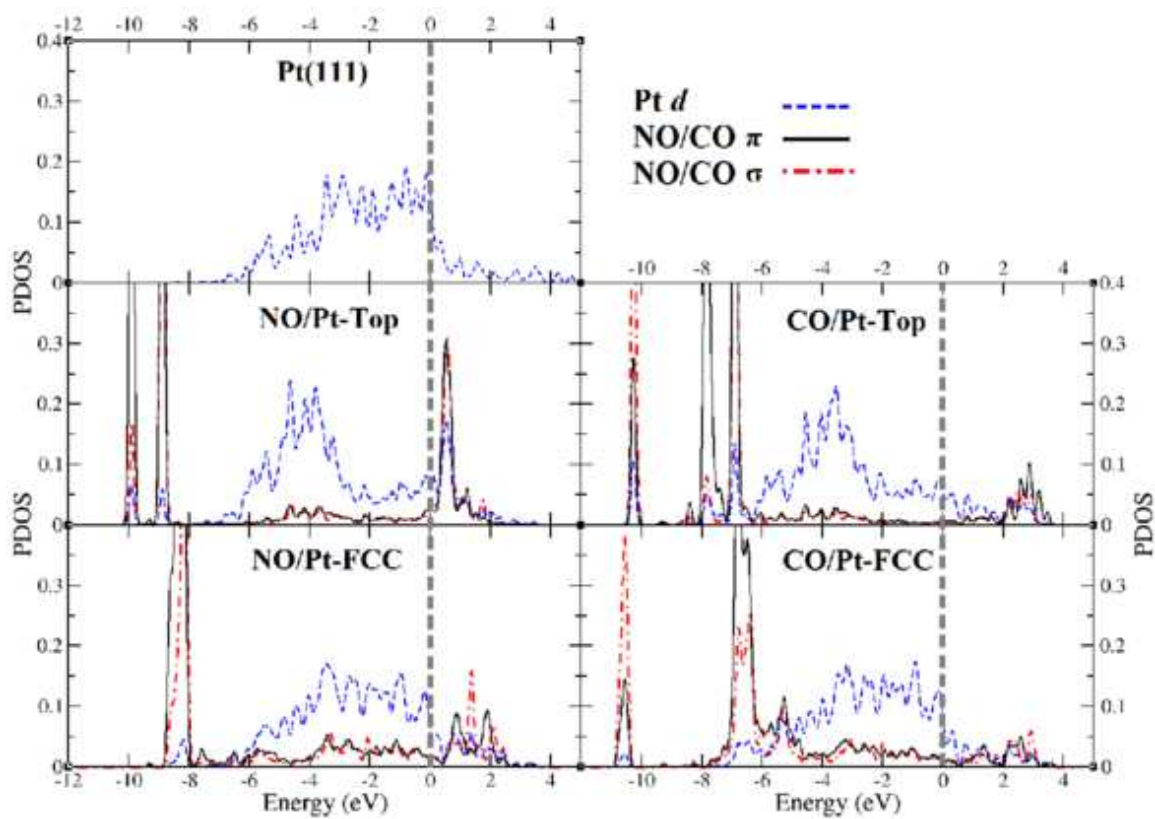


FIG. 3: (Color online) Projected density of states (PDOS) for bare Pt(111) surface and NO and CO adsorption complexes at T_1 and F sites. The π and σ projections are calculated according to the Equations 3 and 4, respectively. The Fermi level is referenced to zero and is indicated by vertical dashed lines in each plot.

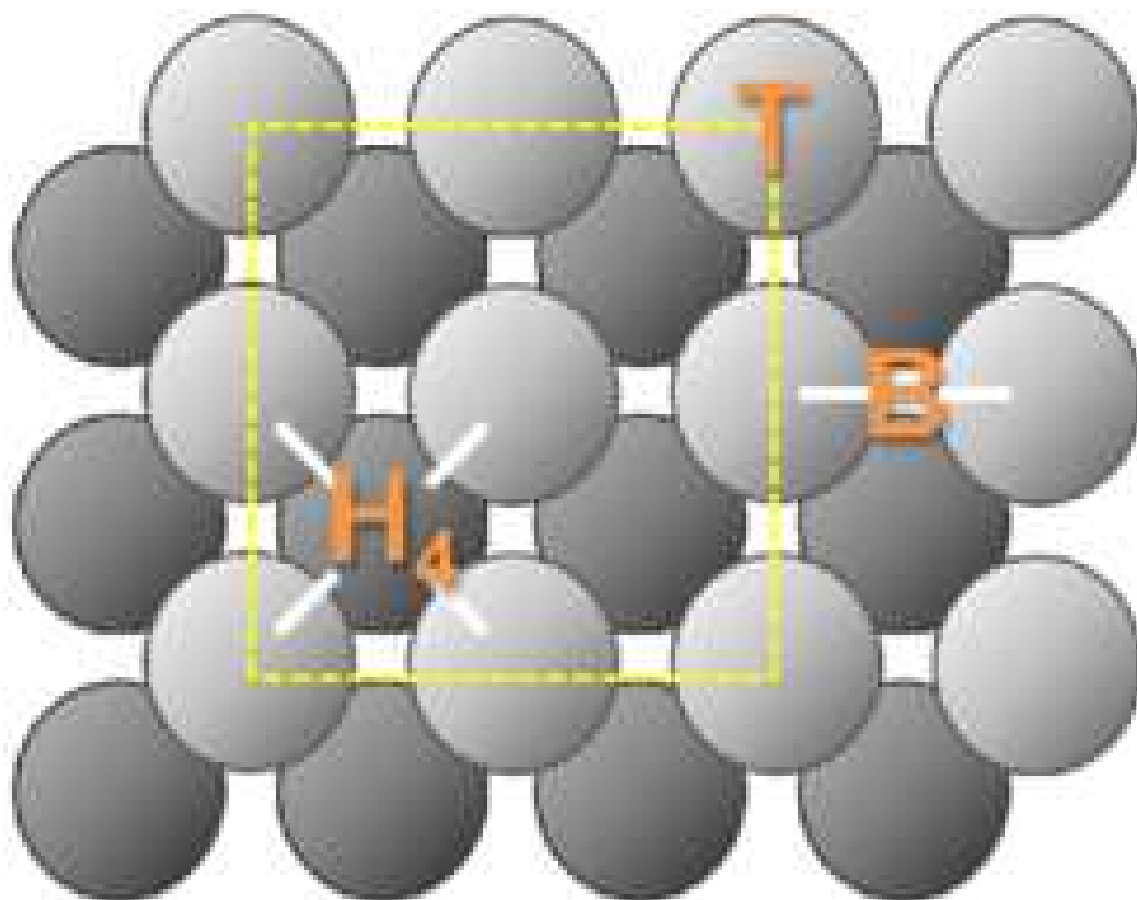


FIG. 4: Top view of the Pt(100) surface. Top (T), bridge (B), and four-fold hollow H_4 adsorption sites are indicated. The employed surface cell is shown by dashed lines.

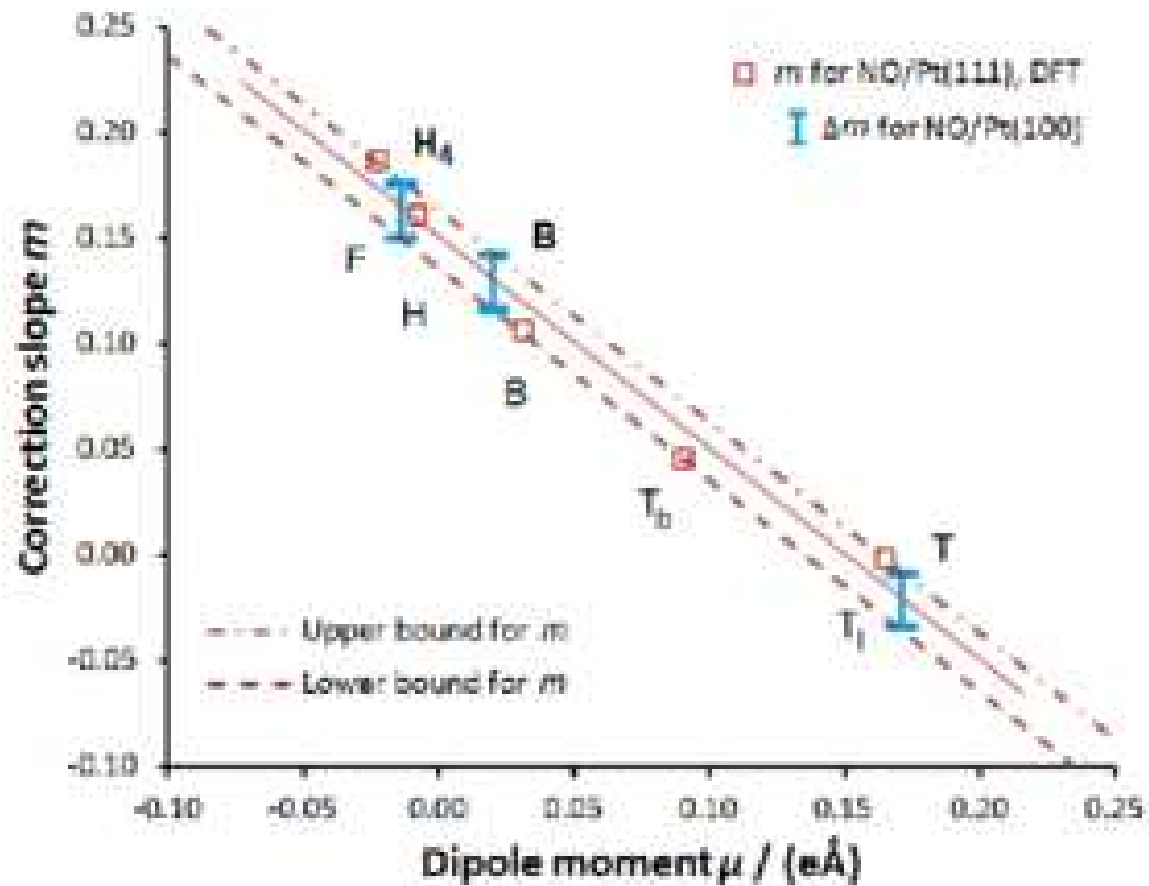


FIG. 5: (Color online) Plot of the correlation between E_{chem} correction slopes and the dipole moment μ calculated using O PSP 1 for the five sites on Pt(111) surface. The NO/Pt(111) DFT data are shown with red crosses. The approximate correction slope m is bound by upper and lower limits shown as red dashed lines. The range for the approximate Pt(100) correction slope values, Δm are shown in blue for three different adsorption sites.

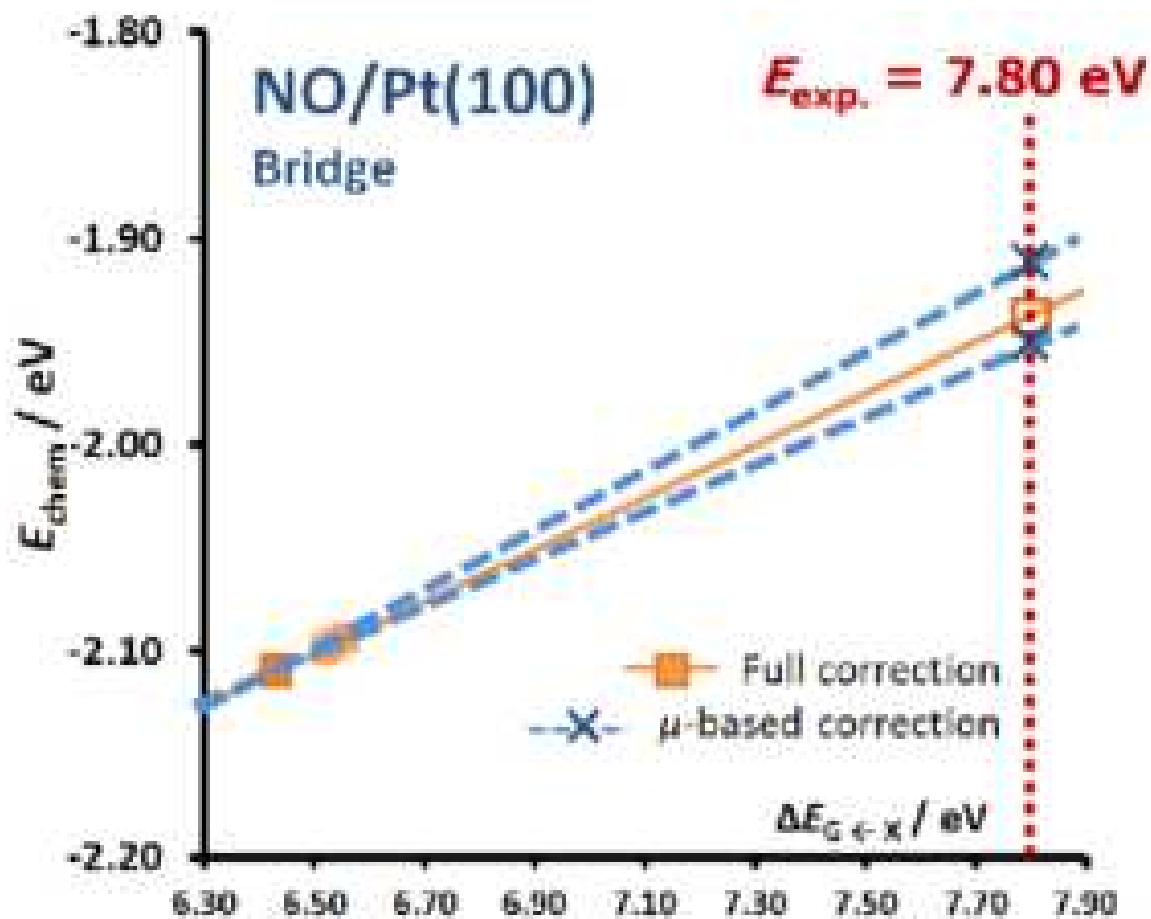


FIG. 6: (Color online) Summary of the μ -based correction method for NO/Pt(100) B site. The two blue dashed lines indicate the trends in E_{chem} vs. $\Delta E_{G \leftarrow X}$ using the upper and lower bound correction slope values from Figure 5. The μ -based correction values for $E_{\text{chem}}^{\text{corr,dip}}$ are shown in blue X's. The uncorrected value of E_{chem} and the corresponding value of $E_{\text{chem}}^{\text{corr}}$ using the full correction scheme are shown in filled and empty orange squares, respectively, connected by a linear fit shown in orange. In all cases, the corrected chemisorption energy value is determined by extrapolating the linear trend to the $\Delta E_{G \leftarrow X}$ value of 7.80 eV.

-
- [1] P. J. Feibelman, B. Hammer, J. K. Nørskov, F. Wagner, M. Scheffler, R. Stumpf, R. Watwe, and J. Dumesic, *J. Phys. Chem. B* **105**, 4018 (2001).
- [2] J. P. Perdew, J. A. Chevary, S. H. Vosko, K. A. Jackson, M. R. Pederson, D. J. Singh, and C. Fiolhais, *Phys. Rev. B* **46**, 6671 (1992).
- [3] J. P. Perdew, K. Burke, and M. Ernzerhof, *Phys. Rev. Lett.* **77**, 3865 (1996).
- [4] B. Hammer, L. B. Hansen, and J. K. Nørskov, *Phys. Rev. B* **59**, 7413 (1999).
- [5] B. Hammer, Y. Morikawa, and J. K. Nørskov, *Phys. Rev. Lett.* **76**, 2141 (1996).
- [6] I. Grinberg, Y. Yourdshahyan, and A. M. Rappe, *J. Chem. Phys.* **117**, 2264 (2002).
- [7] A. Gil, A. Clotet, J. M. Ricart, G. Kresse, M. Garcia-Hernandez, N. Rosch, and P. Sautet, *Surf. Sci.* **530**, 71 (2003).
- [8] G. Kresse, A. Gil, and P. Sautet, *Phys. Rev. B* **68**, 073401 (2003).
- [9] R. A. Olsen, P. H. T. Philipsen, and E. J. Baerends, *J. Chem. Phys.* **119**, 4522 (2003).
- [10] F. Abild-Pedersen and M. P. Andersson, *Surf. Sci.* **601**, 1747 (2007).
- [11] I. Dabo, A. Wieckowski, and N. Marzari, *J. Am. Chem. Soc.* **129**, 11045 (2007).
- [12] S. E. Mason, I. Grinberg, and A. M. Rappe, *Phys. Rev. B* **69**, 161401R (2004).
- [13] M. Lynch and P. Hu, *Surf. Sci.* **458**, 1 (2000).
- [14] L. Mitas, J. C. Grossman, I. Stich, and J. Tobik, *Phys. Rev. Lett.* **84**, 1479 (2000).
- [15] J. C. Grossman, L. Mitas, and K. Raghavachari, *Phys. Rev. Lett.* **75**, 3870 (1995).
- [16] M. Gajdoš, J. Hafner, and A. Eichler, *J. Phys.: Condens. Matter* **18**, 13 (2006).
- [17] S. E. Mason, I. Grinberg, and A. M. Rappe, *J. Phys. Chem. B* **110**, 3816 (2006).
- [18] S. E. Mason, I. Grinberg, and A. M. Rappe, *J. Phys. Chem. C* **112**, 1963 (2008).
- [19] J. W. Bennett, I. Grinberg, and A. M. Rappe, *Phys. Rev. B* **73**, 180102R (2006).
- [20] A. M. Rappe, K. M. Rabe, E. Kaxiras, and J. D. Joannopoulos, *Phys. Rev. B Rapid Comm.* **41**, 1227 (1990).
- [21] N. J. Ramer and A. M. Rappe, *Phys. Rev. B* **59**, 12471 (1999).
- [22] N. Troullier and J. L. Martins, *Phys. Rev. B* **43**, 1993 (1991).
- [23] *Optimized pseudopotential interface / unification module*, <http://opium.sourceforge.net>.
- [24] H. J. Monkhorst and J. D. Pack, *Phys. Rev. B* **13**, 5188 (1976).
- [25] Z. H. Zeng, J. L. F. DaSilva, and W. Z. Li, *Phys. Chem. Chem. Phys.* **12**, 2459 (2010).
- [26] N. U. Zhanpeisov and H. Fukumura, *J. Chem. Theory Comput.* **2**, 801 (2006).
- [27] M. T. M. Koper, R. A. van Santen, S. A. Wasileski, and M. J. Weaver, *J. Chem. Phys.* **113**, 4392 (2000).
- [28] R. B. Getman and W. F. Schneider, *J. Phys. Chem. C* **111**, 389 (2007).
- [29] H. Aizawa, Y. Morikawa, S. Tsuneyuki, K. Fukutani, and T. Ohno, *Surf. Sci.* **514**, 394 (2002).
- [30] D. Loffreda, D. Simon, and P. Sautet, *J. Chem. Phys.* **108**, 6447 (1998).
- [31] D. Loffreda, D. Simon, and P. Sautet, *Chem. Phys. Lett.* **291**, 15 (1998).
- [32] Z. H. Zeng, J. L. F. DaSilva, H. Q. Deng, and W. X. Li, *Phys. Rev. B* **79**, 205413 (2009).
- [33] J. Rempel, J. Greeley, L. B. Hansen, O. H. Nielsen, J. K. Nørskov, and M. Mavrikakis, *J. Phys. Chem. C* **113**, 20623 (2009).
- [34] Q. Ge and D. A. King, *Chem. Phys. Lett.* **285**, 15 (1998).
- [35] C. Popa, C. F. J. Flipse, A. P. J. Jansen, R. A. van Santen, and P. Sautet, *Phys. Rev. B* **73**, 245408 (2006).
- [36] J. A. Herron, S. Tonelli, and M. Mavrikakis, *Surf. Sci.* **606**, 1670 (2012).
- [37] W. P. Krekelberg, J. Greeley, and M. Mavrikakis, *J. Phys. Chem. B* **108**, 987 (2004).
- [38] R. Burch, S. T. Daniells, and P. Hu, *J. Chem. Phys.* **117**, 2902 (2002).
- [39] H. Tang and B. L. Trout, *J. Phys. Chem. B* **109**, 17630 (2005).
- [40] K. P. Huber and G. Herzberg, *Molecular Spectra and Molecular Structure IV. Constants of Diatomic Molecules* (Van Nostrand Reinhold Company, New York, 1979).
- [41] D. C. Ford, Y. Xu, and M. Mavrikakis, *Surf. Sci.* **587**, 159 (2005).
- [42] M. Mavrikakis, J. Rempel, J. Greeley, L. B. Hansen, and J. K. Nørskov, *J. Chem. Phys.* **117**, 6737 (2002).
- [43] K. Honkala, P. Pirilä, and K. Laasonen, *Surf. Sci.* **489**, 72 (2001).
- [44] K. Honkala, P. Pirilä, and K. Laasonen, *Phys. Rev. Lett.* **86**, 5942 (2001).
- [45] K. H. Hansen, Ž. Šljivančanin, B. Hammer, E. Lægsgaard, F. Besenbacher, and I. Stensgaard, *Surf. Sci.* **496**, 1 (2002).
- [46] P. Deshlahra, J. Conway, E. E. Wolf, and W. F. Schneider, *Langmuir* **28**, 8408 (2012).
- [47] Z. H. Zeng, J. L. F. DaSilva, and W. X. Li, *Phys. Rev. B* **81**, 085408 (2010).
- [48] J. Greeley, J. Nørskov, and M. Mavrikakis, *Annu. Rev. Phys. Chem.* **53**, 319 (2002).
- [49] Q. Ge, , and M. Neurock, *J. Am. Chem. Soc.* **2004**, 1551 (2003).
- [50] D. Mei, Q. Ge, M. Neurock, L. Kieken, and J. Lerou, *Mol. Phys.* **102**, 361 (2004).
- [51] D. Mei, J. Du, and M. Neurock, *Ind. Eng. Chem. Res.* **49**, 10364 (2010).
- [52] V. A. Ranea, E. A. Bea, E. E. Mola, and R. Imbihl, *Surf. Sci.* **600**, 2663 (2006).